crystals

MDPI

Article

Effects of the Rare Earth Y on the Structural and Tensile Properties of Mg-based Alloy: A First-Principles Study

Yan Gao [1,*], Chuang Wu [1], Wenjiang Feng [2], Yan He [2], Haisheng He [1], Jingyu Yang [1] and Xiuyan Chen [2]

[1] Experimental Teaching Center, Shenyang Normal University, Shenyang 110034, China; meto085@163.com (C.W.); hehaisheng1002@163.com (H.H.); jingyuyang525@163.com (J.Y.)
[2] College of Physics Science and Technology, Shenyang Normal University, Shenyang 110034, China; fengwj@synu.edu.cn (W.F.); lisaheyan@163.com (Y.H.); chenxy@synu.edu.cn (X.C.)
* Correspondence: gaoy@synu.edu.cn

Abstract: In order to investigate the effect of the rare earth element Y on the strengthening potency of magnesium alloys and its strengthening mechanism under tension. In this paper, the solid solution structures with Y atom content of 1.8 at.% and 3.7 at.% were built, respectively, and their cohesive energies and stress-strain curve were calculated in the strain range of 0–20%. The calculation results of the cohesive energies showed that the structure of element Y is more stable with the increase of strains. The calculation results of stress and strain showed that Y element can improve the yield strength and tensile strength of the Mg-based alloy, and the strengthening effect is better when the Y content is 3.7 at.%.

Keywords: Mg-based alloy; first principles; structural properties; tensile properties

Citation: Gao, Y.; Wu, C.; Feng, W.; He, Y.; He, H.; Yang, J.; Chen, X. Effects of the Rare Earth Y on the Structural and Tensile Properties of Mg-based Alloy: A First-Principles Study. *Crystals* **2021**, *11*, 1003. https://doi.org/10.3390/cryst11081003

Academic Editors: Andreas Hermann and Wojciech Polkowski

Received: 8 July 2021
Accepted: 19 August 2021
Published: 22 August 2021

1. Introduction

In recent years, magnesium alloys have been widely used in aerospace, the automotive industry, computers, the chemical industry and national defense and military industries due to their excellent properties, such as low density, light weight and high specific strength [1–3]. However, the defects of magnesium alloys are also very obvious [4]. The mechanical properties of ordinary magnesium alloys in high temperature environments are not good, which seriously restricts their further development and application [5].

Alloying is the most commonly used among a variety of magnesium alloy strengthening methods [6]. A new type of composite magnesium alloy is formed by adding alloying elements to make it a high-strength, high-toughness, high-performance magnesium alloy [7,8]. Among the many alloying elements of magnesium alloys, rare earth elements perform best [9]. Rare earth elements have the functions of deoxidizing by removing hydrogen and improving casting performance, and also have the ability to enhance alloy strength and high temperature creep resistance [10,11]. In addition, the large size of the rare earth atoms can prevent the α-Mg crystal grains from becoming larger, and help to refine the crystal grains, reduce the tendency of hot cracking due to the looseness of the microstructure, and improve the casting and welding performance of magnesium alloys [12]. Therefore, in recent years, rare-earth magnesium alloys have gradually become a hot spot for development.

The element Y is a widely used rare earth element in heat-resistant magnesium alloys, and it has the same hexagonal close-packed crystal structure as Mg atoms [13]. Magnesium alloy containing Y has the characteristics of high temperature resistance, high plastic toughness and high strength [14]. After the high melting point Y element is added to the magnesium alloy, on the one hand, it can increase the nucleation rate of the alloy and play the role of grain refinement [15], on the other hand, dispersed second-phase particles can be precipitated in the magnesium alloy, which can effectively hinder the movement of dislocations and grain boundary slip. It can improve the creep resistance of magnesium

alloy at high temperature and achieve the purpose of enhancing the strength of magnesium alloy [16,17].

The first-principles tensile test method can calculate the stress value of a crystal structure under different stresses (the stress-strain relationship). The theoretical tensile strength of the crystal structure can be predicted by analyzing the stress value at the yield or fracture of the crystal structure. Wang et al. [18] calculated the stress-strain curves of solid solution structures $Mg_{53}Al$ and $Mg_{51}Al_3$. It was found that the strong covalent bond between Al and Mg and the rearrangement of the electron charge density could improve the tensile strength of the Mg-based alloy, and the $Mg_{51}Al_3$ unit cell could increase the tensile strength of the Mg_{54} unit cell by 9.4%. Zhang et al. [19] calculated and studied the tensile strength of the Al unit cell. The calculation results showed that the theoretical tensile strength of the Al grain boundary was 9.5 GPa at the strain of 16%. Wang et al. [20] calculated the influence of the distribution of Al and Zn atoms on the strength of Mg alloys. It was found that the structure with uniform distribution of alloying elements has greater ideal tensile strength than the structure with separate distribution of alloying elements. Luo et al. [21] calculated the stress-strain curve of Mg-based alloy solid solution in which Al, Zn and Y atoms were dissolved. It was found that the Al, Zn and Y atoms all have a solid solution strengthening effect on the Mg-based alloy, and the Y atom has the best solid solution strengthening effect, which conforms to the experimental rules.

The ideal tensile strength of the crystal structure is an important index parameter to measure material properties and evaluate material quality [22,23]. Therefore, the first-principles tensile calculation method can be used to study the solid solution strengthening effect of alloying elements on Mg-based alloy, and which has an important guiding value for the development and application of magnesium alloys. Considering that the solid solubility of Y atoms in the magnesium alloy does not exceed 3.75 at.%. In this research, $Mg_{53}Y_1$ and $Mg_{52}Y_2$ with Y atom solid solubility of 1.8% at.% and 3.7 at.% were used as the research object. The stress-strain curves and electronic structure changes of the Mg_{54}, $Mg_{53}Y_1$ and $Mg_{52}Y_2$ structures under 0–20% strains were calculated, and the improvement of the yield strength and tensile strength of the Mg-based alloy by the element Y and the strengthening mechanism were analyzed.

2. Computational Methods

The research content in this paper was assembled using the CASTEP software, which is based on the first-principles density functional theory [24,25]. Tensile tests were performed by applying stress to the c-axis direction of the crystal structures of Mg_{54}, $Mg_{53}Y_1$ and $Mg_{52}Y_2$, with a 2% strain increment. In order to obtain accurate stress and strain conditions, the strain interval is 1% between 6% and 10% strain, and the upper limit of the applied strain is 20%. The crystal structure must be geometrically optimized after each strain is applied. The optimize cell option was not checked during the relaxation process, therefore, the lattice constant was not optimized, and only the atomic coordinates in the supercell were optimized. After geometric optimization, the energy, stress and strain values and electronic structure of the supercell structure were calculated.

The CASTEP software parameter setting includes the following contents: Considering that the number of atoms in the unit cell is relatively large, in order not to affect the calculation speed exchange correlation, the function option selects the PW91 functional in the approximate form of GGA. In the convergence setting of the optimized crystal structure, the convergence value of the total energy is 1.0×10^{-5} eV/atom. The convergence value of the force between atoms is 0.03 eV/nm, the maximum internal stress is 0.05 GPa, and the tolerance offset value is set 0.001 Å. In the electronic setting, the cut-off energy is 340 eV, and the number of K points is $3 \times 3 \times 1$. The correlation between particles is set to Ultrasoft super soft pseudopotential. The SCF self-consistent iteration tolerance value is 1.0×10^{-6} eV/atom, the number of convergence steps for geometric mechanism optimization and electronic properties calculation is 150, and the electronic minimizer is set to the default density mixing method and Pulay correction.

3. Results and Discussion

3.1. Structure Properties

As shown in Figure 1a the unit cell of pure magnesium with two Mg atoms has a close-packed hexagonal structure, which space group is P63/MMC, and the lattice constants are a = b = 0.3209 nm, and c = 0.5211 nm. Based on the pure magnesium unit cell and considering factors such as calculation time and accuracy, a 3 × 3 × 3 supercell is built as shown in Figure 1b. The cell contains 54 Mg atoms, and is therefore hereinafter referred to as Mg_{54}, and the corresponding supercell lattice constants are a = b = 0.9628 nm, c = 1.5632 nm. Replacing the magnesium atom at coordinates x = 0.5556, y = 0.4444, z = 0.5833 with an Y atom we obtain the $Mg_{53}Y_1$ crystal structure, that is, a Mg-based alloy solid solution structure with a Y atom content of 1.8 at.%. This structure is shown in Figure 1c. By replacing the magnesium atoms at coordinates x = 0.5556, y = 0.4444, z = 0.5833 and x = 0.5556, y = 0.4444, z = 0.2500 with Y atoms, as shown in Figure 1d, the crystal structure of $Mg_{52}Y_2$ can be obtained, that is, a Mg-based alloy solid solution structure with a Y atoms content of 3.7 at.%.

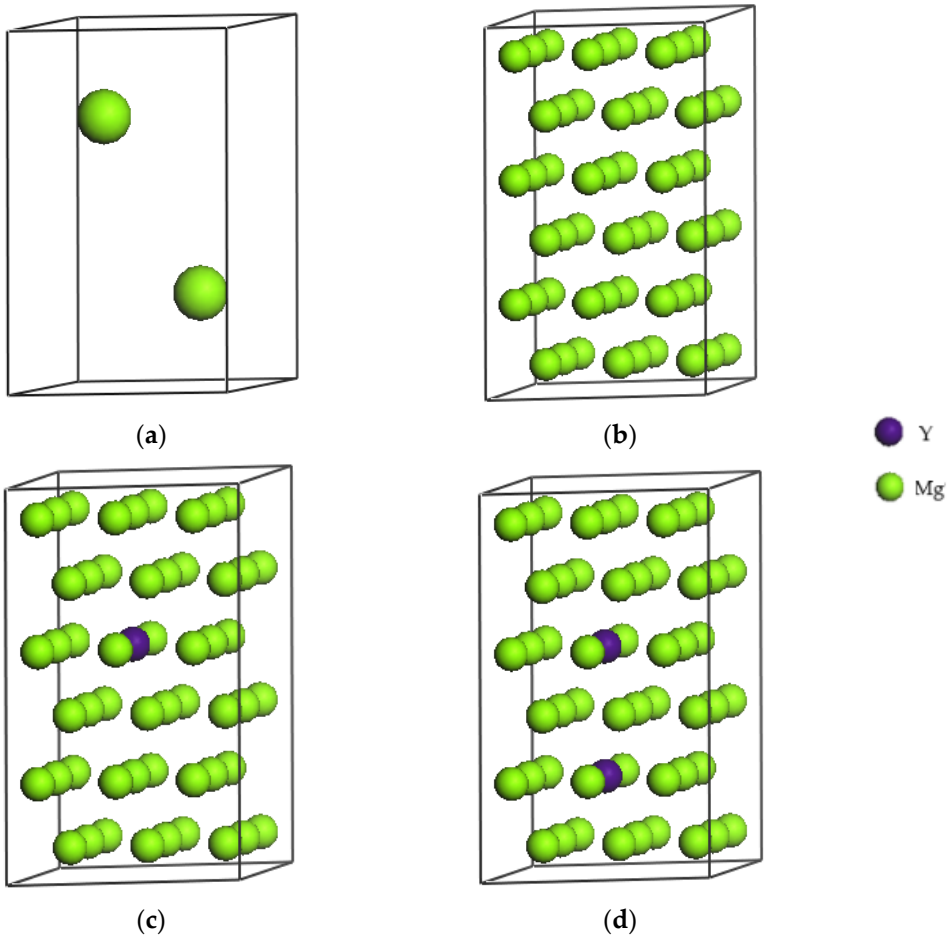

Figure 1. Crystal structures of Mg (**a**), Mg_{54} (**b**), $Mg_{53}Y_1$ (**c**) and $Mg_{52}Y_2$ (**d**).

Based on the Nielsen-Martin calculation method, the first-principles stretching calculation is carried out, and the stress acting on the supercell is the average stress, which can be expressed as [26]:

$$\sigma_{\alpha\beta} = \frac{1}{\Omega}\frac{\partial E_{tot}}{\partial \varepsilon_{\alpha\beta}} \quad (1)$$

In this formula, $\sigma_{\alpha\beta}$ is the average stress acting on the unit cell, Ω is the unit cell volume, E_{tot} is the total energy of the unit cell, and $\varepsilon_{\alpha\beta}$ is the strain tensor. A tensile strain is applied in the direction of the C axis of the unit cell:

$$\varepsilon = \frac{(l_\varepsilon - l_0)}{l_0} \times 100\% \quad (2)$$

In Equation (2), l_0 is the initial cell c-axis length when no strain is applied, and l_ε is the c-axis length of the cell corresponding to the applied strain. It is worth noting that in order to save calculation time, the simulation calculation in this section does not consider the influence of Poisson effect, that is, ignores the influence of tensile strain on the other two axial lattice constants, and considers its value to be fixed.

The stability of the crystal structure depends on its cohesive energy. The definition of binding energy is: if the crystal is split into single free atoms, the work done by the outside world is the cohesive energy of the compound. The cohesive energy of a stably existing compound is negative, and the lower the cohesive energy value, the more stable the crystal structure of the compound. The calculation formula of cohesive energy is as follows [27]:

$$E_{coh} = \frac{E_{tot}^{AB} - N_A E_{atom}^{A} - N_B E_{atom}^{B}}{N_A + N_B} \quad (3)$$

In the above formula, E_{coh} is the cohesive energy of the intermetallic compound, E_{tot} is the total energy of the compound, E_{atom}^{A} and E_{atom}^{B} are the energies of the A and B atoms in the free state, respectively. The free state atomic energyies of Mg and Y are -972.5822 eV/atom and -188.5729 eV/atom, respectively: N_A and N_B are the corresponding numbers of atoms in the unit cell.

The cohesive energy of Mg_{54}, $Mg_{53}Y_1$, and $Mg_{52}Y_2$ at 0–20% strains were calculated, as shown in Table 1. First, the cohesive energy of the three structures are all negative at zero strain, indicating that the three structures can exist stably. Further analysis found that in the range of 0–20% strains, the cohesive energy of the three structures all increase with the increase of strain. Since the larger the absolute value of the cohesive energy, the more stable the structure, so it can be determined that the stability of the three structures decreases with the increase of strain. The reason why the structures become unstable may be the weakening of the chemical bonds between atoms due to stretching. It is worth noting that although the stability of the three structures has decreased, but the cohesive energy values are always negative, indicating that the three structures can still remain stable within the range of 0–20% strains. In addition, it can also be found that the stability of the $Mg_{53}Y_1$, and $Mg_{52}Y_2$ structures are stronger than that of Mg_{54}, and the $Mg_{52}Y_2$ structure is the most stable.

Table 1. The cohesive energy of Mg_{54}, $Mg_{53}Y_1$ and $Mg_{52}Y_2$ under different strains.

Strain (%)	E_{coh}, kJ·mol^{-1}		
	Mg_{54}	$Mg_{53}Y_1$	$Mg_{52}Y_2$
0	−193.46	−199.66	−205.63
2	−193.01	−199.40	−205.52
4	−192.44	−198.95	−205.15
6	−191.70	−198.28	−204.49
7	−191.41	−197.97	−204.33
8	−191.37	−197.74	−204.08
9	−190.90	−197.43	−203.77
10	−190.47	−196.97	−203.32
12	−189.77	−196.15	−202.43
14	−188.75	−195.08	−201.29
16	−187.46	−193.77	−199.92
18	−186.00	−192.32	−198.84
20	−184.60	−190.84	−197.64

3.2. Tensile Properties

In production applications, structural parts often fail due to excessive plastic deformation. For components with strict requirements, plastic deformation is generally not allowed. For components with less stringent requirements, materials are often selected based on the yield strength value σ_s. Under 0–20% strains, the stress values of Mg_{54}, $Mg_{53}Y_1$, and $Mg_{52}Y_2$ solid solution structure are listed in Table 2, and the stress-strain curve is drawn at the same time, as shown in Figure 2. The abscissa represents the applied strains, and the ordinate represents the stress values corresponding to the strains.

Table 2. The Stress values of Mg_{54}, $Mg_{53}Y_1$, $Mg_{53}Y_2$ under different strains.

Strains (%)	Stress, GPa		
	Mg_{54}	**$Mg_{53}Y_1$**	**$Mg_{52}Y_2$**
0	0.00	0.00	0.00
2	1.74	1.23	0.75
4	2.35	1.94	1.83
6	2.69	2.67	2.63
7	1.21	1.49	1.57
8	1.85	1.99	2.04
9	2.22	2.36	2.40
10	2.47	2.76	2.92
12	3.11	3.39	3.65
14	4.15	4.25	4.47
16	4.97	4.93	5.15
18	5.15	5.24	5.63
20	5.02	5.37	4.22

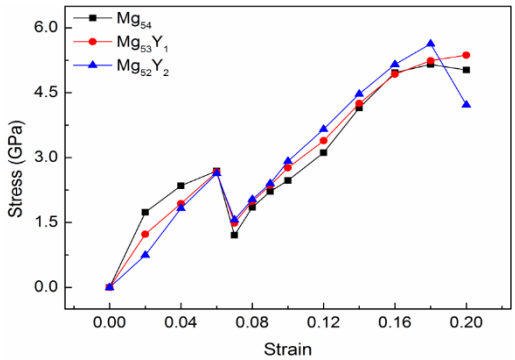

Figure 2. Stress-strain curve of Y Mg_{54}, $Mg_{53}Y_1$ and $Mg_{52}Y_2$.

It can be found from Figure 2 that the three types of structures are all elastic-uneven plastic-uniform plastic deformation types. When the structure is subjected to elastic deformation, obvious upper and lower yield points appear. In the initial stage, when the stress is small, the elongation of the structure changes in proportion to the stress. At this time, the material undergoes elastic deformation after stress, and the material can return to its original length when there is no stress. It can be seen from Figure 2 that the linear variation range of Mg_{54}, $Mg_{53}Y_1$, and $Mg_{52}Y_2$ is very small.

As the stress increases, the tensile strains experienced by the material continues to increase. At this time, both elastic deformation and plastic deformation occur, and it is difficult for the material to fully recover to its original length after the stress is unloaded. When the strain reaches 6%, the upper yield points of the three structures appear at the same time. The upper yield strengths of Mg_{54}, $Mg_{53}Y_1$, and $Mg_{52}Y_2$ are 2.69 GPa, 2.67 GPa and 2.63 GPa, respectively. At the same time, with the application of stress, the lower yield point appears at 7% strain. The lower yield strengths of Mg_{54}, $Mg_{53}Y_1$, and $Mg_{52}Y_2$ are 1.21 GPa, 1.49 GPa, and 1.57 GPa, respectively. For structures with upper and lower yield

points, the lower yield strength is usually selected as the yield strength of the material structure, which is generally expressed by σ_s [28]. The yield strength is a unique strength index for materials with yield phenomena. The yield strengths of $Mg_{53}Y_1$, and $Mg_{52}Y_2$ are higher than that of Mg_{54}, and are increased by 23.14% and 29.75%, respectively, compared to Mg_{54}. It shows that the rare earth element Y can increase the yield strength of Mg-based alloy alloys, and the strengthening effect on Mg-based alloy alloys is stronger when the Y content is 3.7 at.%.

After the material is stretched to the yield stage, there will be a plastic deformation interval, and the resistance of the material against external force stretching will increase with the growth of the plastic deformation, until the stress reaches the tensile strength σ_b [29]. Tensile strength is the ability of a material to resist damage under the action of external force. After reaching the tensile strength, the stress values will decrease as the strains increases. At this time, the deformation strengthening effect of the material structure can no longer compensate for the reduced load-bearing capacity due to the reduction of the cross-section. The tensile strength represents the maximum stress value that a material can withstand under tensile deformation, and which is an important indicator of the material's resistance to tensile deformation. It can be seen from Figure 2 that when the yield strength is reached, several structures begin to undergo plastic deformation. With the gradual increase of strains, the stress values of several structures increase rapidly until the tensile strength is reached. The tensile strength values of Mg_{54}, $Mg_{53}Y_1$, and $Mg_{52}Y_2$ are 5.15 GPa, 5.37 GPa and 5.63 GPa, respectively. It shows that the rare earth Y element can improve the tensile strength of Mg-based alloy alloys, and the enhancement effect is best when the Y content is 3.7 at.%.

Based on the above analysis, it can be found that the Y element can enhance the strength of the Mg-based alloys. When the Y atom content is 3.7 at.%, the strengthening effect is greater than 1.8 at.%. This conclusion is consistent with the experimental results [30]. It was found that the Y element can increases the tensile strength of magnesium alloys, but the plasticity will be decreased. Therefore, although the addition of Y reduces the elastic deformability of the Mg-based alloy. However, both the yield strength and the tensile strength are improved, and the strengthening effect becomes stronger as the solid solubility increases.

4. Conclusions

The first-principles method is used to investigate the effect of rare earth Y element on the tensile properties of Mg-based alloys. Under the strains of 0–20%, the crystal structures of Mg_{54}, $Mg_{53}Y_1$, and $Mg_{52}Y_2$ can all remain stable. The structure of $Mg_{52}Y_2$ is more stable than that of Mg_{54} and $Mg_{53}Y_1$, indicating that rare earth element Y can enhance the stability of Mg-based alloya. When the Y atoms are dissolved in the Mg-based alloy at a content of 1.8 at.% and 3.7 at.%, the yield strength and tensile strength of the Mg-based alloy can be promoted. The theoretical tensile strength values of Mg_{54}, $Mg_{53}Y_1$, and $Mg_{52}Y_2$ are 5.15 GPa, 5.37 GPa and 5.63 GPa, respectively. When the Y atom content is 3.7 at.%, the enhancement effect on the Mg-based alloy is better than 1.8 at.%.

Author Contributions: Writing—original draft preparation, Y.G.; software, C.W., W.F. and Y.H.; writing—review and editing, X.C., H.H. and J.Y.; project administration Y.G. and Y.H.; All authors have read and agreed to the published version of the manuscript.

Funding: This research was funded by the Scientific Research Project of Liaoning Provincial Department of Education, grant number LQN202001; the Liaoning Provincial Natural Science Foundation Program Guidance Plan; grant number 2019-ZD-0484.

Institutional Review Board Statement: Not applicable.

Informed Consent Statement: Not applicable.

Data Availability Statement: Not applicable.

Conflicts of Interest: The authors declare that they have no conflict of interest.

References

1. Patel, H.A.; Chen, D.L.; Bhole, S.D.; Sadayappan, K. Microstructure and tensile properties of thixomolded magnesium alloys. *J. Alloys Compd.* **2010**, *496*, 140–148. [CrossRef]
2. Bakhsheshi-Rad, H.R.; Abdellahi, M.; Hamzah, E.; Ismail, A.F.; Bahmanpour, M. Modelling corrosion rate of biodegradable magnesium-based alloys: The case study of Mg-Zn-RE-xCa (x=0, 0.5, 1.5, 3 and 6wt%) alloys. *J. Alloys Compd.* **2016**, *687*, 630–642. [CrossRef]
3. Kurzynowski, T.; Pawlak, A.; Smolina, I. The potential of SLM technology for processing magnesium alloys in aerospace industry. *Arch. Civ. Mech. Eng.* **2020**, *20*, 1–13. [CrossRef]
4. Wu, M.M.; Jiang, Y.; Wang, J.W.; Wu, J.; Tang, B.Y.; Peng, L.M.; Ding, W.J. Structural, elastic and electronic properties of mg(cu 1 x zn x) 2 alloys calculated by first-principles. *J. Alloys Compd.* **2011**, *509*, 2885–2890. [CrossRef]
5. Wang, M.; Xu, X.Y.; Wang, H.Y.; He, L.; Huang, M. Evolution of dislocation and twin densities in a Mg alloy at quasi-static and high strain rates. *Acta Mater.* **2020**, *201*, 102–113. [CrossRef]
6. Luo, Z.; Chen, X.H.; Song, K.; Liu, C.Q.; Dai, Y.; Zhao, D.; Pan, F.S. Effect of Alloying Element on Electromagnetic Interference Shielding Effectiveness of Binary Magnesium Alloys. *Acta Metall. Sin.* **2019**, *32*, 817–824. [CrossRef]
7. Yang, C.; Pan, F.; Chen, X.; Luo, N. Effects of Sm addition on electromagnetic interference shielding property of Mg-Zn-Zr alloys. *Appl. Phys. A* **2017**, *123*, 400.1–400.7. [CrossRef]
8. Guan, K.; Li. B.; Yang, Q.; Qiu, X.; Tian, Z.; Meng, J. Effects of 1.5 wt% samarium (Sm) addition on microstructures and tensile properties of a Mg-6.0Zn-0.5Zr alloy. *J. Alloys Compd.* **2018**, *735*, 1737–1749. [CrossRef]
9. Zucchi, F.; Grassi, V.; Frignani, A.; Monticelli, C.; Trabanelli, G. Electrochemical behaviour of a magnesium alloy containing rare earth elements. *J. Appl. Electrochem.* **2006**, *36*, 195–204. [CrossRef]
10. Rao, J.; Li, H. Oxidation and ignition behavior of a magnesium alloy containing rare earth elements. *Int. J. Adv. Manuf. Tech.* **2010**, *51*, 225–231. [CrossRef]
11. Tsai, Y.; Chou, C.; Jeng, R.; Lee, S.; Lin, C. Effect of rare earth elements addition on microstructures and mechanical properties of A356 alloy. *Int. J. Cast Metal. Res.* **2011**, *24*, 83–87. [CrossRef]
12. Coy, A.E.; Viejo, F.; Skeldon, P.; Thompson, G.E. Susceptibility of rare-earth-magnesium alloys to micro-galvanic corrosion. *Corros. Sci.* **2010**, *52*, 3896–3906. [CrossRef]
13. Yang, M.B.; Hou, M.D.; Zhang, J.; Pan, F.S. Effects of Ce, Y and Gd additions on as-cast microstructure and mechanical properties of Mg-3Sn-2Sr magnesium alloy. *Trans. Nonferr. Metal. Soc.* **2014**, *24*, 2497–2506. [CrossRef]
14. Gorny, A.; Bamberger, M.; Katsman, A. High temperature phase stabilized microstructure in Mg-Zn-Sn alloys with Y and Sb additions. *J. Mater. Sci.* **2007**, *42*, 10014–10022. [CrossRef]
15. Yang, M.; Pan, F. Effects of Y addition on as-cast microstructure and mechanical properties of Mg-3Sn-2Ca (wt.%) magnesium alloy. *Mat. Sci. Eng. A* **2009**, *525*, 112–120. [CrossRef]
16. Huang, X.; Suzuki, K.; Saito, N. Textures and stretch formability of Mg-6Al-1Zn magnesium alloy sheets rolled at high temperatures up to 793 K. *Scr. Mater.* **2009**, *60*, 651–654. [CrossRef]
17. Chen, H.L.; Lin, L.; Mao, P.L.; Liu, Z. Phase stability, electronic, elastic and thermodynamic properties of Al-RE intermetallics in Mg-Al-RE alloy: A first principles study. *J. Magnes. Alloys* **2015**, *3*, 197–202. [CrossRef]
18. Wang, C.; Han, P.; Zhang, L.; Zhang, C.; Yan, X.; Xu, B. The strengthening effect of Al atoms into Mg-Al alloy: A first-principles study. *J. Alloys Compd.* **2009**, *482*, 540–543. [CrossRef]
19. Zhang, Y.; Lü, G.H.; Deng, S.H.; Wang, T.M. First-principles computational tensile test on an Al grain boundary. *Acta Phys. Sin.* **2006**, *55*, 2901–2907. (In Chinese)
20. Wang, C.; Huang, T.L.; Wang, H.Y.; Xue, X.N.; Jiang, Q.C. Effects of distributions of Al, Zn and Al+Zn atoms on the strengthening potency of Mg alloys: A first-principles calculations. *Comp. Mater. Sci.* **2015**, *104*, 23–28. [CrossRef]
21. Luo, S.Q.; Tang, A.T.; Pan, F.S.; Song, K.; Wang, W.Q. Effect of mole ratio of Y to Zn on phase constituent of Mg-Zn-Zr-Y alloys. *Trans. Nonferr. Metal. Soc.* **2011**, *21*, 795–800. [CrossRef]
22. Tong, L.B.; Li, X.H.; Zhang, H.J. Effect of long period stacking ordered phase on the microstructure, texture and mechanical properties of extruded Mg-Y-Zn alloy. *Mater. Sci. Eng. A* **2013**, *563*, 177–183. [CrossRef]
23. Giusepponi, S.; Celino, M. The ideal tensile strength of tungsten and tungsten alloys by first-principles calculations. *J. Nucl. Mater.* **2013**, *435*, 52–55. [CrossRef]
24. Mao, P.; Yu, B.; Liu, Z.; Wang, F.; Ju, Y. First-principles calculations of structural, elastic and electronic properties of AB_2 type intermetallics in Mg-Zn-Ca-Cu alloy. *J. Magnes Alloys* **2013**, *1*, 256–262. [CrossRef]
25. Mao, P.L.; Yu, B.; Liu, Z.; Wang, F.; Ju, Y. Mechanical, electronic and thermodynamic properties of Mg_2Ca Laves phase under high pressure: A first-principles calculation. *Comp. Mater. Sci.* **2014**, *88*, 61–70. [CrossRef]
26. Gironcoli, S.D.; Baroni, S.; Resta, R. Piezoelectric properties of III-V semiconductors from first-principles linear-response theory. *Phys. Rev. Lett.* **1989**, *62*, 2853–2856. [CrossRef] [PubMed]
27. Wang, F.; Sun, S.J.; Wang, Z.; Yu, B.; Mao, P.L.; Liu, Z. Microstructure, mechanical properties and first-principle analysis of vacuum die-cast Mg-7Al alloy with Sn addition. *Rare Metals* **2015**, *15*, 1–7. [CrossRef]
28. Jing, Z.; Zhang, X.; Li, W.; Pan, F.; Guo, Z. Partition of Er among the constituent phases and the yield phenomenon in a semi-continuously cast Mg-Zn-Zr alloy. *Scr. Mater.* **2010**, *63*, 367–370.

29. Lin, L.; Chen, L.; Liu, Z. Tensile strength improvement of an Mg-12Gd-3Y (wt%) alloy processed by hot extrusion and free forging. *J. Mater. Sci.* **2008**, *43*, 4493. [CrossRef]
30. Zheng, A. Effect of Rare Earth Y Content on Microstructure and Mechanical Property of Mg Alloy. *Hot Working Technol.* **2016**, *4*, 40–42. (In Chinese)